

Received 16 November 2022, accepted 30 November 2022, date of publication 2 December 2022,
date of current version 21 December 2022.

Digital Object Identifier 10.1109/ACCESS.2022.3226654

RESEARCH ARTICLE

An Effective Falcon Optimization Algorithm Based MPPT Under Partial Shaded Photovoltaic Systems

MUHANNAD J. ALSHAREEF¹

Department of Communication and Electronics Engineering, College of Engineering in Al-Qunfudhah, Umm Al-Qura University, Mecca 21955, Saudi Arabia
e-mail: mjshareef@uqu.edu.sa

ABSTRACT Uncertain conditions involving partial shading can be found in large-scale solar photovoltaic (PV) systems. There is a possibility that the performance of the PV system will suffer as a result of partial shading conditions (PSCs) because it creates multiple peaks in the power–voltage (P–V) characteristics. Nevertheless, for the photovoltaic system to be utilized in the most effective manner, it needs to be run at a global maximum power point (GMPP). A new strategy based on the falcon optimization algorithm (FOA) is introduced in this paper for the tracking of GMPP. The perturb and observe (P&O) and the particle swarm optimization (PSO) techniques have certain drawbacks that can be resolved using a new optimization method known as the FOA. These limitations include a lower convergence speed and steady-state oscillations. The tracking performance of the proposed method is evaluated and compared to that of three MPPT algorithms, namely grey wolf optimization (GWO), PSO and P&O, for a PV array that is functioning under PSCs and displaying numerous peaks. An implementation of the proposed FOA-MPPT algorithm on a PV system was carried out with the help of MATLAB/SIMULINK. Simulation tests conducted under a variety of partial shading patterns reveal that the proposed FOA outperforms all three MPPT algorithms: GWO, PSO, and P&O. Simulation results show that the MPPT efficiency of FOA in four different partial shading conditions is 99.93%, 99.82%, 99.80%, and 99.81%. Furthermore, the simulation results show that the tracking time of proposed FOA in four different partial shading conditions is 0.4 s, 0.41 s, 0.39 s, and 0.41 s, respectively. Moreover, the proposed FOA is tested using actual and measurable data from Neom, Saudi Arabia. According to the simulation results, the proposed FOA generates significantly more revenue than other compared algorithms.

INDEX TERMS Falcon optimization algorithm (FOA), maximum power point tracking (MPPT), partial shading conditions (PSCs), photovoltaic (PV) system.

I. INTRODUCTION

Modern power grids have solar photovoltaic (PV) installed as their most promising energy source [1]. The advancement of this technology is based on the availability of the solar resource and the necessity of reducing one's carbon footprint. Nevertheless, power output of PV generation, is extremely dependent on environmental conditions, such as the temperature of PV cells and solar irradiance. Also, the optimal power extraction from solar energy is hampered by PV systems' nonlinear P-V curve [2]. Therefore, maximum power point tracking (MPPT) algorithms must be included in all PV

systems. The MPPT process is an optimization technique that adjusts the PV to supply the most possible power to the load. Additionally, there are a myriad of reasons that lower the efficiency with which PV converts energy into usable form. In addition, there are a number of power losses associated with PVs due to partial shading from the sun. Due to the fact that the current generated by a solar array's panels varies depending on the amount of shade they are subjected to, bypass diodes are normally linked at the panels' corresponding outputs to reverse bias (disable) those panels generating the lowest current in a hierarchical manner (in accordance with the load's power demand). As a result, the MPPT problem becomes non-convex because these diodes cause multiple power peaks in the power- voltage (P-V) curve.

The associate editor coordinating the review of this manuscript and approving it for publication was Yonghao Gui¹.

When PV panels are exposed to full insolation, the MPPT problem is convex; as a result, multiple traditional optimization algorithms [3], [5], [6] have been presented to optimize the PV array for maximum output power. However, due to their restricted ability to explore, these algorithms most often merge to local maxima under partial shading conditions (PSCs).

When the ambient temperature and solar insolation fluctuate, an MPPT scheme should adapt to get the most out of the PV system. The process of maximum power point tracking (MPPT) is compounded by nonlinear current-voltage (I-V) characteristics and a power-voltage (P-V) curve that varies greatly in line with variations in solar insolation and temperature. Examples of well-known classical MPPT methods are hill climbing (HC) [7] and perturb and observe (P&O) [4], [8], [9]. Both techniques lead to power loss because of oscillations around MPP brought on by the perturbation's constant up-and-down movement. Although the INC method [10] mitigates these fluctuations, it does not eliminate them entirely.

Under conditions of constant solar irradiance and temperature, and only a single MPP in the P-V curve, the MPPT techniques introduced by several researchers [11], [12] are optimal. On the other hand, large PV installations with multiple PV modules connected in series and/or parallel are not excellent fits for these techniques.

If even one module in a PV system is not performing as expected, it can drag down the entire system. Partial shading conditions (PSC) can occur when the PV array receives uneven amounts of sunlight from factors like passing clouds or nearby objects casting shadows. PSC causes a drop in output power of the PV system, the degree of which varies with system configuration and shading pattern (SP). Due to the multiple peaks appearing in the P-V curve that PSC causes, conventional MPPT methods are unable to compensate for the loss of power that results from PSC. This is because it cannot distinguish between global and local peak. Methods exist to mitigate the decrease in power output caused by PS; these include rearranging PV arrays [13], implementing intricate converter circuit topologies [14], and optimizing MPPT [15]. The use of a better MPPT algorithm is the most appealing option because it does not require any structural changes to an existing system. Therefore, many MPPT methods have been developed to deal with GMPP under PSC [16]. Both fuzzy logic [17] and artificial neural networks (ANNs) [18] are forms of intelligent control that rely heavily on input data. Particle swarm optimization (PSO) [19], [20], the firefly algorithm [21] the artificial bee colony algorithm, the gray wolf optimization (GWO) [22] and the bat algorithm [23] are just some of the swarm intelligence algorithms that have been used to keep track GMPP. Because of how easy they are to create and put into practice, these algorithms are able to follow the GMPP while PSC is active, with no oscillation around the GMPP. The PSO, like any basic metaheuristic algorithm, needs to be properly initialized and tuned on a regular basis to achieve optimal tracking performance. Inadequate

performance is the direct result of sloppy initialization and tuning of the system's parameters. For instance, due to the attribute's tendency to decrease randomness when scanning for the optimal candidate, the tracking time and convergence speed for particles with a large size are both relatively slow [24]. Instead of using traditional metaheuristics, bioinspired optimization approaches take their cues from the collective intelligence of natural phenomena such as swarms, flocks, herds, and schools of animals. These strategies use firefly, bee, and bird behaviors in MPPT algorithms. Cuckoo search (CS) [25], the flower pollination algorithm [24], [26] the ABC, the firefly algorithm, the fractional chaotic ensemble PSO [27], wind-driven optimization [28], improved differential evolution (DE) [29], genetic algorithm (GA) [30], cat swarm optimization [31], and the sliding mode control [32], are all examples of well-known bioinspired optimization methods. According to several scholars [25], [31], [33] the proposed algorithm's drawbacks arise from the computational burden imposed by the exploring mechanism's complexity. In contrast to this proposed method, the drawbacks of [34], [35], wherein the complex nature of the structure, formula, and principle leads to early oscillation and tracking time issues during GMPP tracking are less severe.

Based on the flower pollination algorithm (FPA) and the P&O method, [36] presented a hybrid MPPT. Utilizing chaos maps, other researchers [37], [38] improved the FPA's efficiency. To identify the GMPP throughout PSC, [39] employed an enhanced leader adaptive velocity PSO. Five series-connected modules were subjected to the bat algorithm (BA) proposed by [40] which involved multiple shade patterns. For four series-connected modules in five different PSC, [35] utilized grass hopper optimization (GHO). [41] developed an adaptive particle swarm optimization (APSO) based MPPT system for five series-connected shaded modules. Various optimization strategies, such as the enhanced leader particle swarm optimization (ELPSO) aided by P&O [36] and the wind driven optimization algorithm (WOA) [28], have been presented for interconnected PV systems. Compared to the bio-inspired algorithm proposed in this paper, other algorithms [24], [31], [38] take more than 0.5 s to track the GMPP and are thus much slower. Multiple hybrids of traditional MPPT and soft computing MPPT are presented in the literature, including PSO mixed with ANFIS [42], Fuzzy mixed with PSO [43], ACO mixed with P&O [44], PSO mixed with P&O [45], and PSO mixed with DE [46]. Good results and potential applications have been found for these combinations. Although the proposed methods in this paper have a simple concept as well as structure, MPP tracking using a mix of traditional and new forms of computing. The MPPT approaches need extensive amounts of computer programming in addition to high implementation costs and computational complexity.

In an effort to counteract those shortcomings, the current work proposes for the first time in the context of PV-MPPT application a novel MPPT algorithm based on the falcon optimization algorithm (FOA). The falcon's hunting technique

served as inspiration for the proposed metaheuristic algorithm [47], the falcon optimization algorithm (FOA) is a robust and reliable algorithm for solving stochastic population-based problems; it has three stages of action settlement and needs to call for adjustments to a number of parameters. The proposed method was inspired by the chase technique used by falcons when searching for prey in the air. Falcons are secretive birds whose hunting strategies vary with their individual needs. However, distinctive strategies emerge, and remarkable models retain fundamental assumptions about the flying journey. According to work by Tucker [48], [49] falcons are the most proficient fliers among birds. Because FOA requires less work in parameter tuning than other MPPT approaches, the author was inspired to incorporate it, and it is easy to put into practice. Also essential to its success is a search mechanism with three stages that allows for rapid convergence. The authors made good use of the benefits of the FOA method to build a robust MPPT technique that is quick to respond and highly reliable. Further, the author was convinced that they could modify the approach so that it works well with MPPT applications. In this paper, four sets of PSC are assessed using software simulation to determine the efficiency of the FOA based MPPT in a wide range of environmental conditions. The obtained results were then compared to those obtained by using the GWO, PSO and P&O methods. The dominance of FOA is demonstrated through a comparative evaluation of other methods across multiple aspects. When compared to metaheuristic algorithms, the proposed FOA is able to decrease the initial oscillation that occurs through the tracking process. This contributes to a low loss of energy, improves tracking performance, and makes it easier to track real global MPP and minimize the oscillation that occurs around the GMPP. The proposed FOA contains a straightforward search mechanism that demonstrates good MPPT performance in the presence of different PSCs. As a result, the power extracted from the PV panel can be increased. The results of the proposed FOA are validated by intensive simulation work in order to demonstrate the efficiency as well as the benefits of the method. In a general sense, the following are the most significant contributions made by this work

- The FOA a novel and straightforward bio-inspired optimization method, is proposed for tracking the global maximum power point (GMPP). it features GMPP tracking with a low energy loss, a quick convergence speed, good accuracy, simple control scheme, and easy implementation. The proposed FOA has been shown to be effective in a variety of environmental conditions.

- The proposed FOA method is evaluated against the standard P&O and many other well-known metaheuristics in terms of tracking speed and accuracy of tracking, Simulation results are used to verify the proposed FOA's functionality and effectiveness.

The reminder of the paper is laid out as follows. Section II, covers the basics of solar PV modelling, and demonstrates the effect of the PSCs on the functionality of the PV solar array and in Section III, introduces the FOA, a novel bioinspired

method. Section IV presents the comprehensive steps of the FOA-MPPT implementation. Simulation studies involving a variety of PSCs are analyzed in Section V. Section VI, provides a thorough comparison of the proposed method with different soft computing methods in the literature. Section VII, presents a performance evaluation analysis of FOA with the regard to the amount of energy saved, revenue generated, and net energy yield. Section VIII, summaries the final conclusions.

II. PHOTOVOLTAIC MODELS

The PV system under study is shown in Fig 1 together with the DC-DC boost converter and the battery. Numerous researchers place a high value on PV cell modelling because of the significant impact that nonlinear characteristics and variations in environmental conditions have on PV cell performance. It is possible to create an accurate PV cell using either a single or double diode model. The single-diode model (SDM) is widely used because it is straightforward to implement and requires fewer parameters than alternative models [50]. Current source is denoted by I_{ph} , while series and parallel resistances are denoted by R_s and R_{sh} accordingly indicating contact and leakage losses. The sum of the currents produced by PV cells can be calculated using kirchhoff's current law (KCL) applied to the equivalent circuit, as shown in (1).

$$I = I_{ph} - I_o \left[\exp \left(\frac{V + IR_s}{aV_t} \right) - 1 \right] - \frac{V + IR_s}{R_{sh}} \quad (1)$$

where PV current, leakage current, are denoted by I_{ph} and I_o , respectively. It can be expressed as $V_t = Ns k T q$, where V_t and a stand for the thermal voltage and the ideality factor of a diode D , respectively. In this equation, k represents the Boltzmann constant, and its value is 1.38×10^{-23} J/K. T represents the temperature of a photovoltaic cell in Kelvin, and q and N_s represent the charge of an electron (1.6×10^{19} C) and the number of cells in series, I_{ph} and I_o can both be determined by applying (2) and (3).

$$I_{ph} = [I_{ph\ STC} + k_i (T - T_{STC})] \frac{G}{G_{STC}} \quad (2)$$

where k_i represents the coefficient of short circuit current and $I_{p,STC}$ represents the PV current under standard test conditions (STC), which are defined as 25°C and 1000W/m^2 , respectively.

$$I_o = \frac{I_{SC,STC} + k_v (T - T_{STC})}{\exp \left(\frac{V_{OC,STC} + k_v (T - T_{STC})}{n v_T} \right) - 1} \quad (3)$$

where k_v represents the coefficient of open circuit voltage, $I_{SC,ST}$ represents the short circuit current under STC, and $V_{SC,ST}$ represents the open circuit voltage under STC. One can rewrite Eq.(1) as Eq.(4) to determine the total current produced by a PV module when subjected to a partial shading effect.

$$I = N_{pm} \left\{ I_{ph} - I_o \left[\exp \left(\frac{V + IR_s}{aV_t N_{sm}} \right) - 1 \right] \right\} - \frac{V + IR_s}{R_{sh}} \quad (4)$$

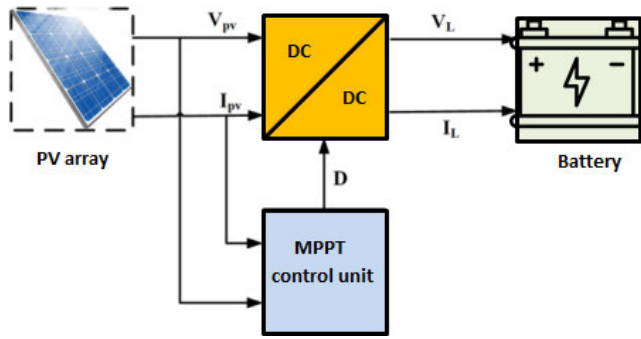


FIGURE 1. A schematic representation of the PV system.

Number of PV modules connected in parallel and in series, respectively, denoted by N_{pm} , and N_{sm} .

A. EFFECT OF PARTIAL SHADING CONDITIONS

PV modules are linked in series and parallel in order to generate enough power for the plant’s intended use [51]. Also, not all PV panels receive the same amount of irradiation due to factors like passing clouds, building shadows, and dust. Partial shading is the result of this unequal irradiance [50]. The current drawn by the shaded PV panel would be equal to the current drawn by the rest of the PV string in this situation. Furthermore, the PV panel that is shaded tends to lose its ability to produce current, and the temperature of that panel rises, leading to hot-spots ultimately damaging the PV panels. A bypass diode across each panel can solve this problem. The author in this paper considered four distinct patterns over a set of four PV panels wired in series (4S), all of which were constructed using a Sharp NT-180/4 U PV module, in order to better comprehend the impact of partial shading. Table 1 displays the PV module’s detailed specifications.

To prevent the flow of current in the reverse direction, a blocking diode is wired into each string. In Fig. 2(a), there are four different patterns

1.) In the first Pattern1, there is no shading at all. With this setup, each of the PV panels (M_1, M_2, M_3 , and M_4) will receive the same amount of sunlight ($1000W/m^2$). Each PV panel has the potential to produce the same amount of current. As a result, it creates a P-V curve where the global maximum power point (GMPP) is held in a single peak. The single peak in the P-V curves of Fig.2(b) is denoted by P_1 .

2) Pattern 2: represents a condition of partial shading where Module M_1 , receives $1000W/m^2$, Module M_2 receives $100W/m^2$, and modules M_3, M_4 receives $300W/m^2$ and $200W/m^2$ of irradiation respectively. The amount of current produced by the PV string is equivalent to the amount of current produced by the PV modules that are shaded because of the presence of shade. In addition, having a bypass diode across each panel will assist in bypassing the maximum current produced by un-shaded PV panels. Because of this disparity in currents, four distinct peaks to appear in the PV curves, which are denoted by the symbols P_2, P_3, P_4 and P_5 in Fig. 2.(b). In Pattern 2, the points P_2, P_3, P_4 are referred to

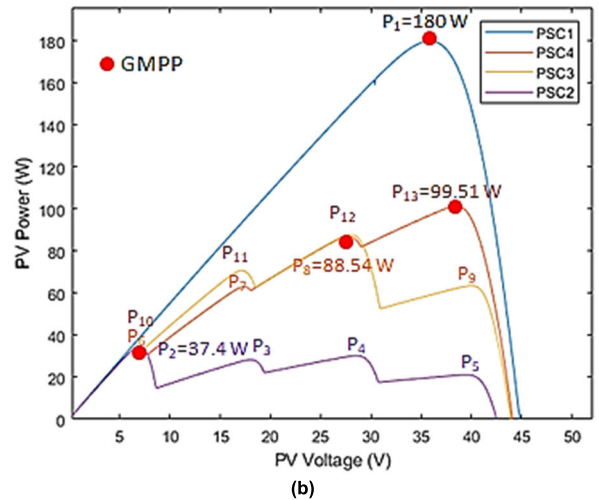
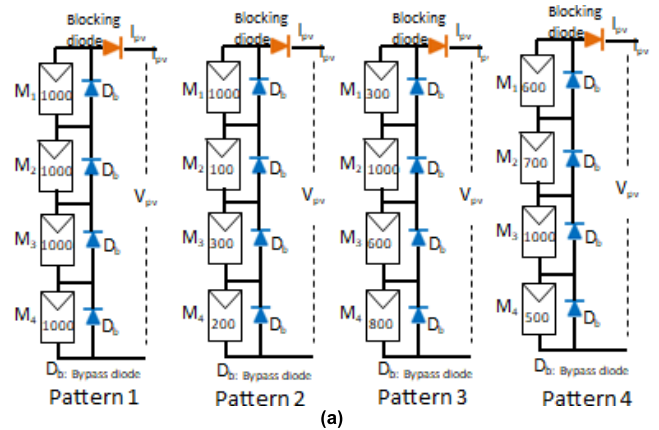


FIGURE 2. Evaluation of partial shading PV module (a) shading patterns, and (b) P-V curve.

as the local maximum power point (LMPP) and the point P_2 is referred to as GMPP.

3) Pattern 3: the photovoltaic modules M_1, M_2, M_3 , and M_4 in this configuration are supplied with $1000W/m^2, 700W/m^2, 500W/m^2$, and $300W/m^2$ of sunlight, respectively. Each of the four photovoltaic modules receives one of four different shades; consequently, each panel generates its own current based on the shade it receives. This causes multiple peaks to appear in the P-V curves. In Fig, 2(b), its points are denoted by the letters P_6, P_7, P_8 , and P_9 respectively. Within these four peaks, there is only one point that is regarded as GMPP, and that point is P_8 . The other points are regarded to be LMPP. As a consequence, there are multiple peaks over the P-V curves due to the conditions of partial shade. The existence of multiple peaks will make it very hard for conventional MPPT algorithms to attain GMPP. The power generating capacity may drop by a significant amount if these algorithms track the LMPP instead of GMPP, which has a negative impact on the PV system’s performance. Therefore, the author in this paper developed a novel MPPT technique to track maximum power regardless of any PSC or patterns.

4) Pattern 4: each panel creates its own current dependent on the shades it collects. As a consequence of this, the

P-V curves display numerous peaks. In Fig. 2(b), its points are indicated by the letters P_{10}, P_{11}, P_{12} , and P_{13} , in that order. P_{13} is the only position among these four peaks that is considered the GMPP. The remaining points are considered to represent LMPP.

III. FALCON OPTIMIZATION ALGORITHM (FOA)

Metaheuristics are algorithms that take their cues from nature and can be used to find approximate solutions to computationally challenging optimization problems. Animal swarming behaviour patterns (such as those of the ant, cuckoo [52], bee, pigeon, bat, and so on have been employed in metaheuristics [53]. Identity, illation-free tools, flexibility, and the ability to avoid local optimums are just a few of the remarkable characteristics underlying metaheuristics [54]. A falcon’s hunting habits inspired the metaheuristic algorithm proposed by [47]. The falcon optimization algorithm (FOA) is a robust method for solving stochastic population-based problems; it consists of a three-stage process that requires adjustments to a number of parameters. The proposed method was inspired by the hunt technique used by falcons when they are in flight in search of their prey. Reclusive falcons adapt their hunting strategies to their specific food needs. Therefore, unique strategies emerge, and incredible models retain presumptions about the flight. Tucker claims that among birds, falcons are the most proficient fliers. In different stages of elevated hunting, the fitting objectives are examined to determine whether or not they exceed the boundaries of flying achievement [48]. Stoops have been observed to approach speeds that are greater than 200 miles per hour (320 kilometers per hour), making the falcon one of the most rapid animals on the planet. Falcons are able to take easy breaths thanks to the presence of a series of small tubercules in their beaks. These direct the flow of air through high-velocity stoops. The majority of hunting takes place during the course of the day (including morning and night). Most of their prey consists of smaller and medium-sized birds, but they will also eat insects like grasshopper, worms, locusts, and crickets [55]. The falcon flies in a variety of routes to get to its prey. The first part of each route is a logarithmic spiral, during which the falcon maintains its head perfectly straight and eyes focused on the prey with extreme accuracy; the second part is a straight segment, during which the falcon flies directly forward towards the prey and dives when the prey is in its vision. Therefore, the process by which a falcon achieves locomotion can be broken down into three stages. Stage 1: involves the falcon looking for prey; stage 2: involves the falcon enhancing its dive by means of a logarithmic spiral; and stage 3: involves the actual diving of the falcon itself, which may or may not result in the successful capture of prey. In any other circumstance, a falcon is quick to change its action in response to the experiences it has had. Fig. 3 presents a graphical illustration of the flying path taken by a falcon during a hunt.

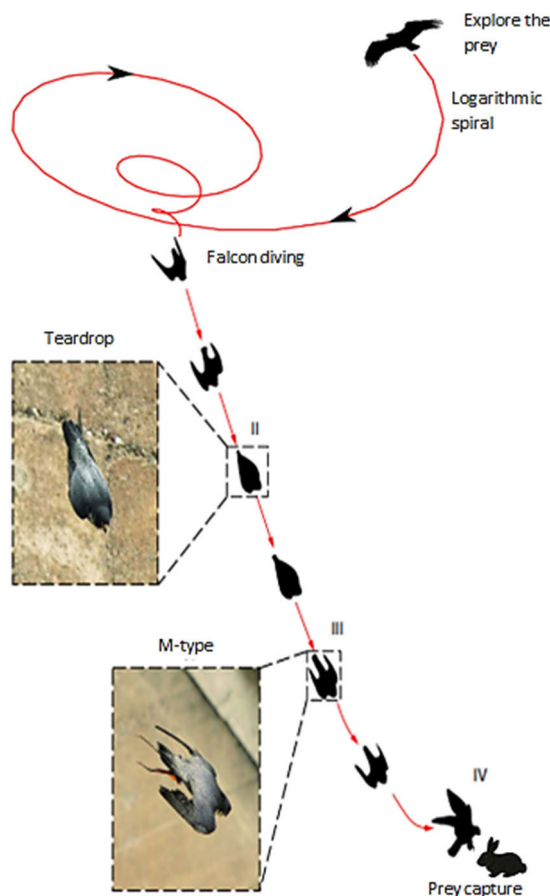


FIGURE 3. A representation of a falcon’s flight route during a hunt.

IV. IMPLEMENTED OF FOA INTO MPPT APPLICATION

The FOA represents a new category of algorithms that take inspiration from the natural world. The PV power is used as the objective function and the duty ratio D of the DC/DC converter serves as the position of the falcon. Fig. 4 presents a flowchart of the proposed falcon optimization algorithm (FOA), and the different steps required to put the FOA method to use in an MPPT application are described as follows

Step 1: Setup the initial problem data and control parameter adjustments. Constraints, decision variables, and the optimization problem are all laid out. Then, the adjustable FOA parameters, including the number of falcons (NP), the values of the cognitive coefficient (c_c), social coefficient (s_c), the maximum speed (v_{max}), following constants (f_c), the awareness probabilities (AP) and dive probabilities (DP) are presented.

Step 2 (Initialize Position and Velocity of the Falcons): The boundary conditions will determine the falcons’ initial velocities and locations in a D -dimensional space, with each falcon’s location defined with respect to the total number of NP applicants in that space. In an MPPT application, the duty cycle d is chosen as the falcon’s agent. The following equation can be used to ensure that the searching area is

initially divided fairly between each searching agent (duty cycle d).

$$d_0^k = \frac{k}{(ss + 1)} \quad (5)$$

where d_0^k represents the falcon's (duty cycle) initial position with order k in the swarm, and ss is the size of the swarm.

The speeds are chosen at random from between the maximum and minimum values of V , which are respectively defined as follows

$$V_{max} = 0.1 \times ub \quad (6)$$

$$V_{min} = -V_{max} \quad (7)$$

where ub represents the maximum value (each dimension's boundary area).

Step 3 (Assess Fitness and Identify Global and Individual Best Positions): Here, the DC/DC converter is operated through its available duty ratios (falcon positions) in rapid succession. The instantaneous PV power output is utilized as a measure of optimum position of each duty cycle d to the prey. This process is done with each duty cycle d , and with respect to MPPT, the objective fitness function (f) is given as:

$$f(d) = \max P_{PV}(d) \quad (8)$$

The fitness value for each falcon is determined. The best overall solution is then assigned to the g_{best} position, while X_{best} position is given to the best position attained by each individual falcon. With the logic that governs the move that occurs behind the dive and awareness probability in mind, the selected positions are used to generate new ones. FOA-based MPPT aims to maximize PV output power. The output power from PV is measured using the PV voltage and PV current.

Step 4 (Generate New Positions and Update the Falcon Positions): In the beginning, two random numbers, known as r_{AP} and r_{DP} , are produced for each falcon using a uniform distribution so that they can be compared with the awareness and dive probabilities. If r_{AP} is less than the awareness probability AP , the falcon makes a movement indicative of its search for prey, taking into account its own and other falcons' past experiences as follow:

$$X_{iter+1} = X_{iter} + V_{iter} + c_s r (X_{best} - X_{iter}) + s_s r (g_{best} - X_{iter}) \quad (9)$$

where X_{iter} and V_{iter} represent the falcon's present position and velocity. The presented algorithm is very much like the search carried out by the PSO algorithm.

If the awareness probability AP , is lower than r_{AP} , then dive probability DP can be compared with r_{DP} , if DP is lower than r_{DP} , the falcon will then select one of the targets as its prey (X_{chosen}), marking the successful completion of the fundamental step in the hunting process. A logarithmic spiral can be obtained from through:

$$X_{iter+1} = X_{iter} + |X_{chosen} - X_{iter}| \times \exp^{bt} \cos(2\pi t) \quad (10)$$

where b is a constant that defines the condition of the spiral logarithm has a value of 1, and t is a variable between -1 and 1 that indicates how close the next position of the falcon would be to the true target.

In the event that DP is larger than r_{DP} , the fitness value (of) of the selected prey is evaluated in relation to the fitness value (of) of the falcon, and the prey that is determined to be the fittest is the one the falcon will chase after, in a manner analogous to a dive step:

$$X_{iter+1} = X_{iter} + V_{iter} + f_c r (X_{chosen} - X_{iter}) \quad (11)$$

If not, the falcon will keep flying from where it is in the optimal position:

$$X_{iter+1} = X_{iter} + V_{iter} + c_c r (X_{best} - X_{iter}) \quad (12)$$

The new position is then tested for velocity and boundary conditions. Following this, the X_{best} and g_{best} values are updated to represent the new fitness levels. The phenomenon of klepto-parasitism between falcons is included in all procedures described in Step 4, while examining a single candidate solution. Because of this, every generation, one falcon can look at other falcons to be potential targets, even prey, for the various movements it performs.

Step 5 (The Determination of Convergence): The optimization process is terminated once a predetermined number of iterations have been completed or when all falcons position changes are less than a predetermined threshold. At this point, the duty cycle at which the DC/DC converter operates is used as output in order for it to be able to track GMPP.

V. SIMULATION RESULTS

A MATLAB/Simulink environment is used to model and examine the proposed FOA-MPPT method. Fig. 1 shows a block diagram of the PV system's modelling, which displays the PV array, DC-DC converter and the MPPT controller. The circuit component parameters values can be shown in Table 2. In this setup, four individual PV modules are linked in series to create the arrays. The DC-DC boost converter MPPT algorithm's sampling time is set to 0.01 s since it is critical that MPP readings are obtained once the system has reached the steady-state condition. This value is selected to account for the transient response of the MPPT inputs, such as the PV voltage and PV current, in order to prevent a delay in the tracking of maximum power and avoid failure. The simulations in Figs. 5 to Fig.8 demonstrate that PV system is tested under different PSCs.

The inductance is determined so that the inductor current I_L is a steady and never goes to zero, allowing the converter to function in continuous current mode (CCM). This means that the minimum value of inductor L is determined as [56]:

$$L = \frac{V_{in} \times (V_{out} - V_{in})}{\Delta i_L \times f_s \times V_{out}} \quad (13)$$

where V_{in} denotes the typical input voltage, V_{OUT} is the desired output voltage, and Δi_L represents estimated inductor ripple current (20% to 40% of the output current).

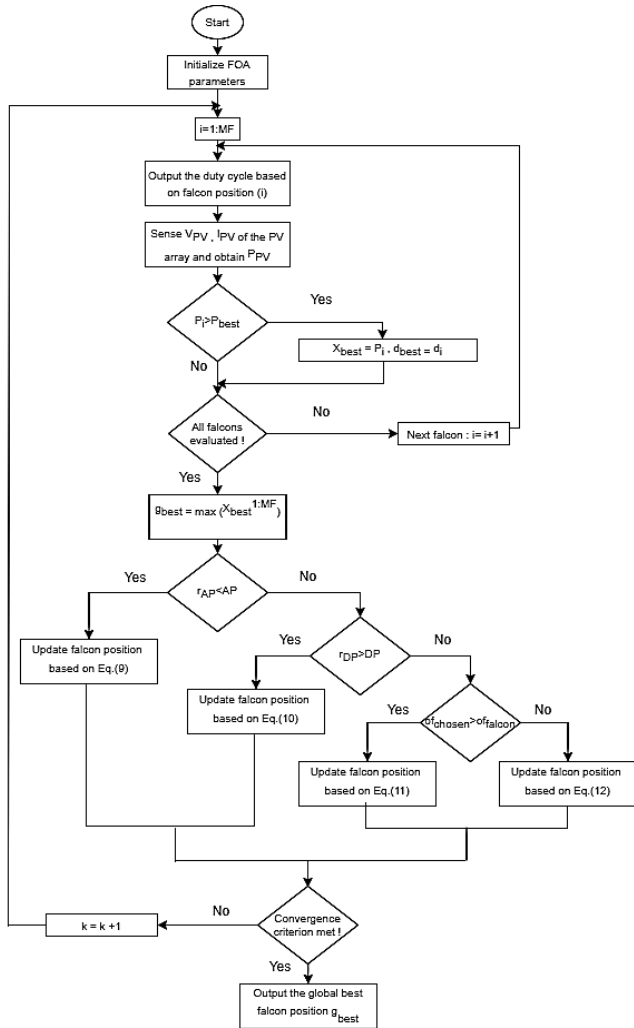


FIGURE 4. Flowchart of the proposed falcon optimization algorithm.

The following formulae can be used to change the values of the output capacitors in order to get the required level of ripple in the output voltage [56]:

$$C_{OUT(min)} = \frac{I_{OUT(max)} \times D}{f_s \times \Delta V_{out}} \quad (14)$$

where $C_{out(min)}$ is the minimum output capacitance, $I_{out(max)}$ is the maximum output current of the application, and ΔV_{out} is desired output voltage ripple.

A. PERFORMANCE EVALUATION

The effectiveness of the MPPT methods is evaluated using the following three indicators:

1) Tracking Efficiency η

$$\eta = \frac{P_m}{P_{MPP}} \times 100\% \quad (15)$$

where P_m is the actual maximum output power and P_{MPP} is the theoretical maximum output power.

2) Tracking Time T

T is the amount of time it takes for the photovoltaic system to attain a stable PV output. One way to

TABLE 1. Specification of PV module [57].

Specification of single PV module	Values
Maximum Power at MPP (P_{mpp})	45 W
Open Circuit Voltage (V_{oc})	11.2 V
Maximum Voltage at MPP (V_{mpp})	8.96 V
Short Circuit Current (I_{sc})	5.6 A
Maximum Current at MPP (I_{MPP})	5.02 A
Configuration of PV module	4-Series

measure it is by counting the number of sampling cycles.

3) Tracking the Rate of Success σ

$$\sigma = \frac{N_{st}}{N_s} \times 100\% \quad (16)$$

where the number of times that the target was successfully tracked, denoted by N_{st} , and the number of simulated times is denoted by N_s . The requirement for determining whether or not the MPPT method was effective in tracking is whether or not it was able to successfully track the GMPP and fits the following criteria:

$$\eta \geq 95\% \quad (17)$$

$$\frac{|V_m - V_{mpp}|}{V_{mpp}} \leq 0.02 \quad (18)$$

V_m refers to the voltage that is actually produced, while V_{MPP} is the voltage that is theoretically expected at MPP.

Table 3 shows the irradiance profile for the several patterns employed in this study.

B. ANALYZING SPECIFIC CASES

1) CASE 1

As shown in Fig. 2(b), there are no LMPPs in Case 1 with GMPPs of 180W. Fig. 5 displays the tracking waveforms generated by the four MPPT methods. The proposed FOA method is shown to have the highest tracking efficiency (99.93%) out of the other MPPT methods tested, with PV output power of 179.9W, and complete convergence towards GMPP occurring in 0.4s. With a PV output power of 179.81W and a tracking efficiency of 99.88%, the GWO method tracks the GMPP in 0.81s. With a PV output power of 179.75W and a tracking efficiency of just 99.85%, the PSO method takes almost 1s to attain the GMPP.

The entire tracking process takes only 0.59s with the P&O method, and its accuracy reaches up to 98.88% as a result of continual oscillation that appears around the GMPP. Hence, the FOA method has the quickest tracking speed.

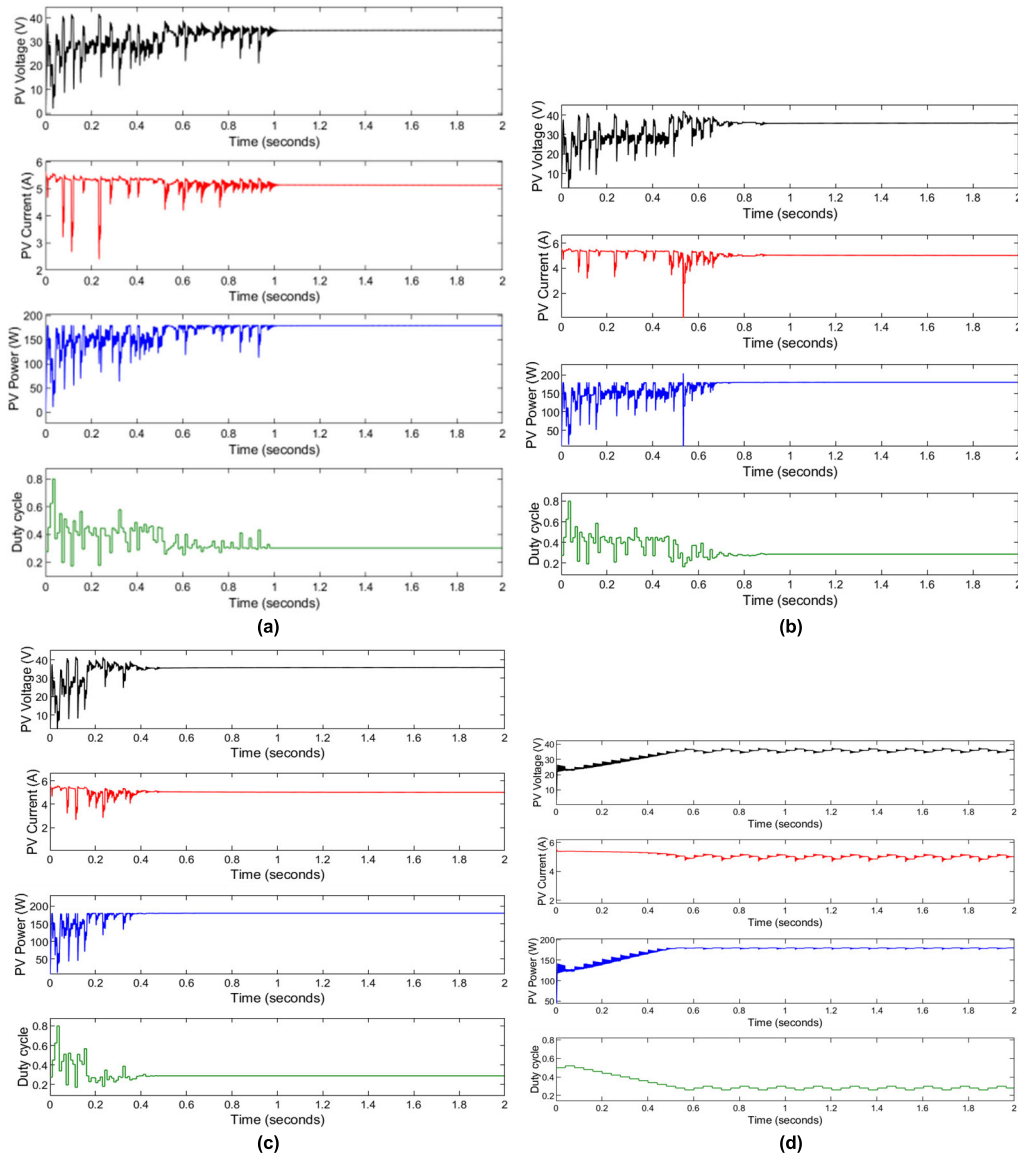


FIGURE 5. Simulation waveforms under case 1 of the (a) PSO method (b) GWO method (c) FOA method (d) P&O method.

TABLE 2. Specification of parameters of circuit component.

Specification of single PV module	Values
Input Voltage at MPP (V_{in})	44.1 V
Output Voltage at MPP (V_{out})	48 V
Switching Frequency (f_s)	20 kHz
L	400 μ H
C_{in}	1 mF
C_{out}	1 mF

2) CASE 2

As can be shown in Fig. 2(b), there are three LMPPs in Case 2 with GMPPs of 37.4W. (b). Fig. 6 displays the tracking

TABLE 3. Irradiance profile for various patterns.

Pattern No.	Irradiation profile in W/m^2
Pattern1	$G_1=1000, G_2=1000, G_3=1000, G_4=1000$
Pattern2	$G_1=1000, G_2=100, G_3=300, G_4=200$
Pattern3	$G_1=300, G_2=1000, G_3=600, G_4=800$
Pattern4	$G_1=600, G_2=700, G_3=1000, G_4=500$

waveforms generated by the four MPPT methods. The proposed FOA method follow the GMPP with tracking efficiency 99.82%, has PV output power of 37.34W and with tracking time of 0.41s. GWO method required a longer tracking time of in 0.9s and has tracking efficiency of 99.49%. With a PV output power of 37.21W. The PSO method shows excessive

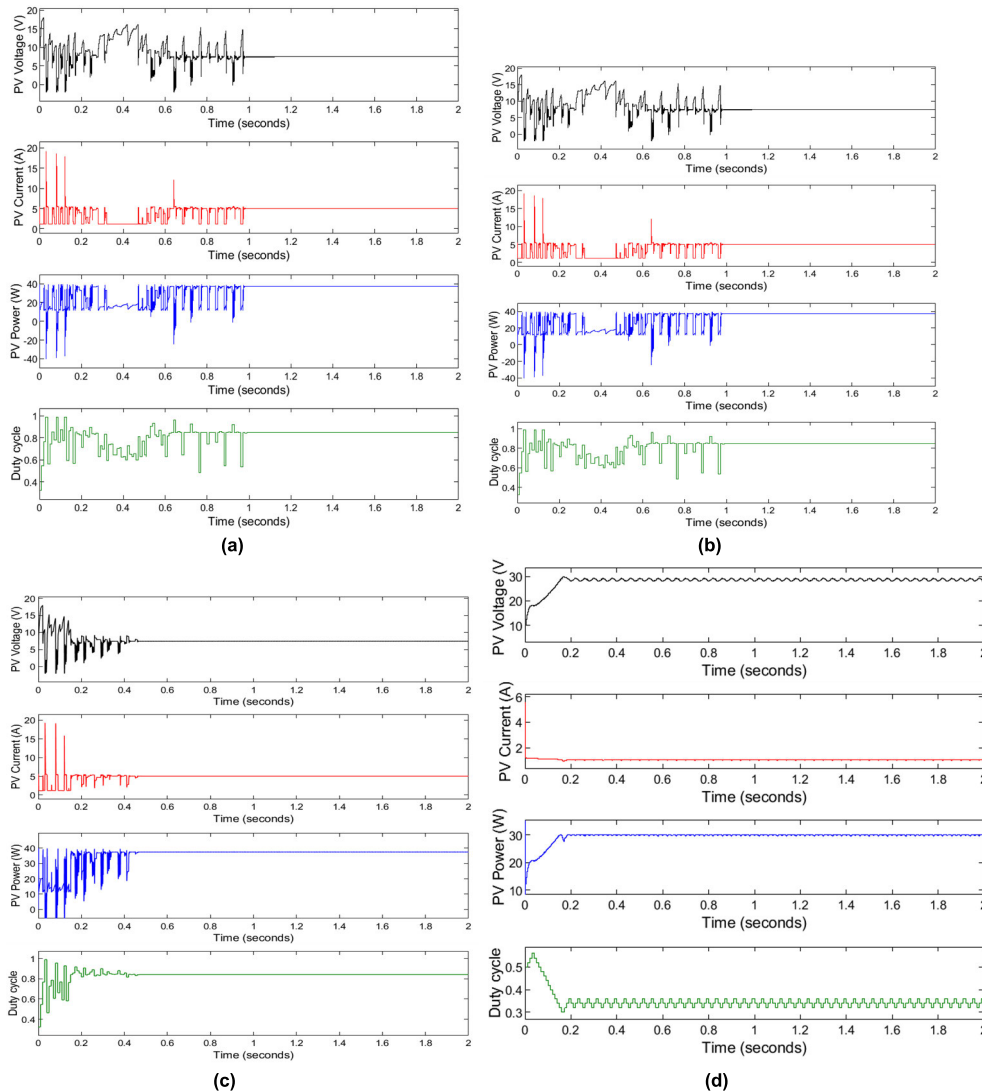


FIGURE 6. Simulation waveforms under case 2 of the (a) PSO method (b) GWO method (c) FOA method (d) P&O method.

oscillation toward convergence to GMPP with tracking time of 1.1s and tracking efficiency of 98.23%, Although the P&O method had quick convergence time of roughly 0.4s, it was unable to identify the GMPP, and it ended up settling at the LMPP (29.32W) with tracking efficiency of 78.39%.

3) CASE 3

As shown in Fig. 2(b), there are three LMPPs in Case 3 with GMPPs of 88.54W. Fig. 7 displays the tracking waveforms generated by the four MPPT methods. The proposed FOA method successfully tracks the GMPP with a short time of 0.39s and tracking efficiency of 99.80%, and has PV output power of 88.37 W. The GWO method converges to the GMPP within 0.7s and has a tracking efficiency of 99.77%. With a PV output power of 88.34 W. The PSO method shows a longer convergence time toward the GMPP with 1.1s and tracking efficiency of 99.75%. Although the P&O method

has successfully identified the correct GMPP at this time, it still demonstrates oscillation around the GMPP. It has a tracking efficiency of 94.77%, PV output power of 83.63 W, and tracking time of 0.38s.

4) CASE 4

As shown in Fig. 2(b), there are three LMPPs in Case 4 with GMPPs of 99.51W. Fig. 8 displays the tracking waveforms generated by the four MPPT methods. The proposed FOA method converges to the GMPP within 0.41s, has a tracking efficiency of 99.81%, and a PV output power of 99.32W. The GWO method reaches the GMPP within 0.9s, which is longer than the aforementioned method, and has a tracking efficiency of 99.74%. With a PV output power of 99.26W, the PSO method tracks the GMPP in 1.35s with a tracking efficiency of 99.70%. With a PV output power of 99.21 W. However, the P&O method gets stuck at LMPP. It has a

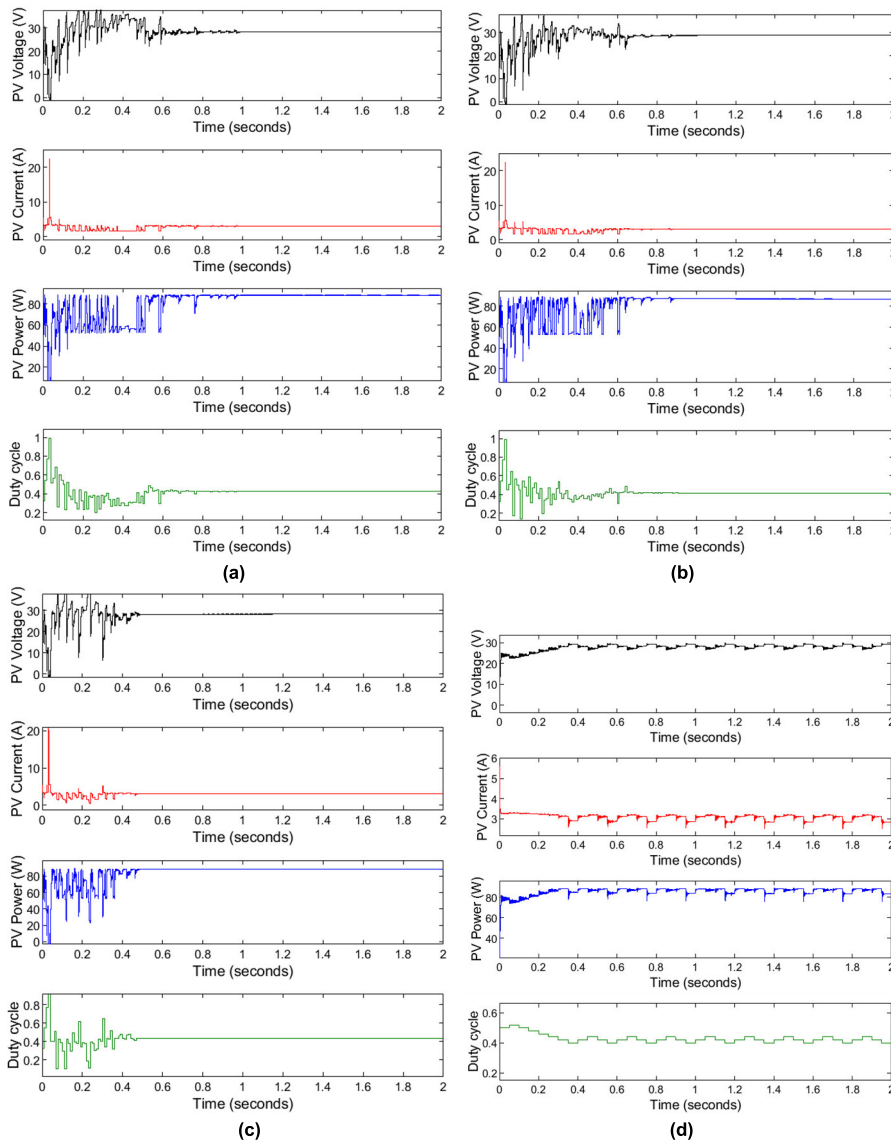


FIGURE 7. Simulation waveforms under case 3 of the (a) PSO method (b) GWO method (c) FOA method (d) P&O method.

tracking efficiency of 53.88% and a PV output power of 53.62W.

The tracking curves shown from Fig. 5 to Fig. 8 indicate that although the GWO method and PSO method guarantee global convergence, this takes a long time. Hence, PSO and GWO methods causes a significant amount of power loss. In addition, fluctuations appear in the PV power waveform when GWO and PSO-based search continue for a longer period of time. Even though the P&O method has a short convergence time, it usually fails to detect the GMPP, and PV output power oscillations continue even after reaching the steady-state condition.

Based on the simulation results presented in Figs. 5-8, the FOA can outperform the GWO, PSO, and P&O methods in terms of faster convergence to GMPP, minimal steady-state

oscillations, and higher tracking efficiency. This is demonstrated by the fact that the FOA is able to effectively deal with any PSC. Table 4 provide a summary of the simulation results. The tracking efficiency given in the tables is computed as the ratio of the average power production from the PV array while it is in the steady-state condition to the maximum power available from the PV array under given pattern. Thus, the FOA-based MPPT performs better than the other three MPPT methods.

5) SUMMARY

Analysis of these four cases demonstrates that the proposed FOA method seems to have the best overall performance of the four MPPT methods, maintaining ideal tracking ability while achieving high tracking efficiency in a relatively short

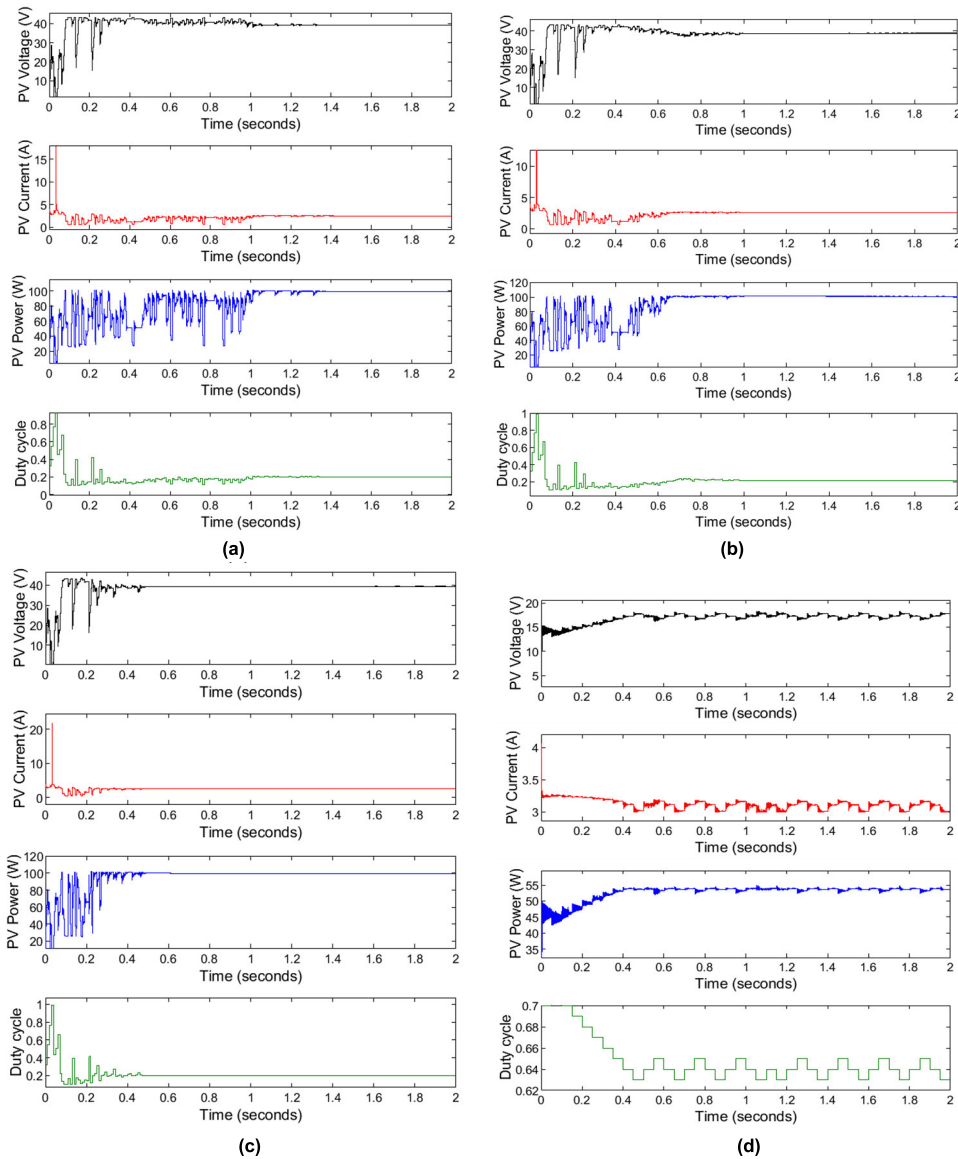


FIGURE 8. Simulation waveforms under case 4 of the (a) PSO method (b) GWO method (c) FOA method (d) P&O method.

amount of time. The data show that the proposed FOA method excels at handling complex PSCs.

VI. COMPTSTIVE STUDY OF THE PROPOSED FOA WITH DIFFERENT SOFT COMPUTING METHODS IN THE LITERATURE

A. QUALITATIVE ANALYSIS

Over the last few decades, new methods have been developed for MPPT applications, and some of these have the potential to reach a GMPP, even under the case of PSC. The contribution of a variety of methodologies that have been proposed for the performance enhancement of PV systems have helped to make the positive impact of environmentally friendly methods of power generation more obvious in recent years. A comparative assessment between the FOA method

and other methods that have been developed in the MPPT is carried out in order to gain a better understanding of the contribution that the FOA method has made to the field of MPPT application. Specifically, the six most important criteria that determine the system’s performance are evaluated, and a bar chart based on the findings of the study is displayed in Fig. 9. The following is a list of the several parameters that explored for the study: ability to track GMPP under PSC, convergence speed, switching stress, robustness, ability to track MPP under normal condition, and dependence on individual panels. It is clear that the FOA method has a robust bar chart. More importantly, the chart information allows the following rankings to be assigned to the different methods: FOA, GWO, PSO, ANN, P&O, in that order. Being able to make a direct, qualitative comparison of a large number of other methods

TABLE 4. Performance comparison of the four MPPT Methods under four PSCs.

Shading Pattern	Algorithm	Voltage at MPP (V)	Current at MPP (A)	Power at MPP (W)	Tracking Time (s)	Tracking Efficiency(%)
Pattern1	P&O	37.3	4.7	177.9	0.58	98.88
	PSO	35.3	5.01	179.75	1	99.85
	GWO	34.5	5.21	179.81	0.81	99.88
	FOA	34.95	5.15	179.9	0.4	99.93
Pattern2	P&O	29.42	0.99	29.32	0.38	78.39
	PSO	7.9	4.65	36.74	1.1	98.23
	GWO	7.41	5.04	37.21	0.9	99.49
	FOA	7.42	5.03	37.24	0.41	99.82
Pattern3	P&O	29.36	2.84	83.63	0.38	94.77
	PSO	28.37	3.10	87.33	1.1	99.75
	GWO	28.36	3.11	87.34	0.7	99.77
	FOA	28.37	3.11	87.37	0.39	99.80
Pattern4	P&O	17.82	3.01	53.62	0.43	53.88
	PSO	38.2	2.60	99.21	1.35	99.70
	GWO	38.4	2.59	99.26	0.9	99.74
	FOA	38.4	2.58	99.32	0.41	99.81

TABLE 5. Ranking of the FOA according to Friedman ranking test.

Algorithm	Friedman Ranking at Pattern1	Friedman Ranking at Pattern2	Friedman Ranking at Pattern3	Friedman Ranking at Pattern4	Overall Ranking
FOA	1	1.25	1.25	1	1
PSO	3.25	3.25	3.5	3	3
P&O	3.5	3.25	3	3.5	4
GWO	2.25	2.25	2.25	2.5	2

the Friedman ranking tests, were carried out in order to examine the performance of each MPPT algorithms.

A nonparametric Friedman ranking test was performed to decide where the proposed algorithm lies in the overall rankings. The outcomes of the Friedman ranking test are presented in Table 5, which reveals that the proposed FOA algorithm beat other algorithms when it came to tracking the GMPP under different patterns.

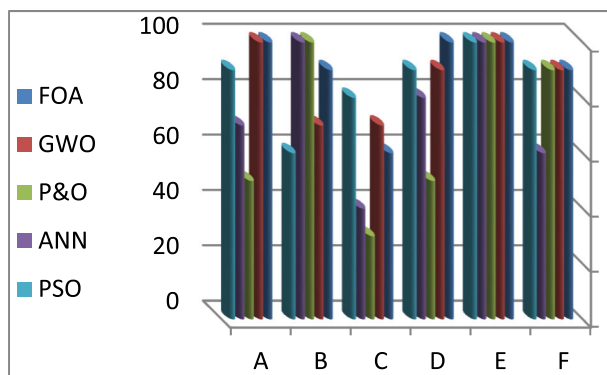
A nonparametric method for comparing the results obtained from two distinct approaches is known as the Wilcoxon rank-sum assessment. The presence of the null hypothesis indicates that there is no discernible difference between the ranks produced by the various techniques of comparison. The alternative hypothesis examines the question of whether or not the outcomes of the comparative technique may be classified according to rank. At this point, a significance level of 5% was used to the Wilcoxon rank sum calculation.

The sign “+” indicates that the FOA algorithm was significantly better than the other algorithm, the sign “≈” indicates that the FOA algorithm had performance that was comparable to the other algorithm, and the sign “-” shows that the FOA algorithm performed poorly when compared to the other algorithm. Table 6 presents the statistical findings that were derived by evaluating all four methods in accordance with the aforementioned four patterns.

VII. RESULTS OF THE DAY-BY-DAY SIMULATION

Saudi Arabia is a country exposed to a significant quantity of solar irradiation on its land and has a high average number of hours of daylight throughout the year, particularly during the months of June, July, and August. For the purposes of this study, data relating to Neom City is analyzed. This data is utilized as input in this section for the software MATLAB/Simulink, which is used to calculate the total power that could be produced from photovoltaic systems. This solar atlas is shown in Fig. 10. Fig. 11 shows the monthly average solar irradiation observed at Neom for each month in the year 2021.

The goal of the method is to identify GMPP during shadows caused by obstructions on rooftops that are present in the environment. Even when such obstructions are continually existing at or near to the position of the PV system, it is possible that they do not cause shadow on a daily basis. This is due to the fact that the presence of a shadow is also dependent on



A-Ability to track GMPP under PSC, B-Convergence speed, C-Switching stress, D-Robustness, E- Ability to track MPP under normal condition, F- Dependence on individual panels

FIGURE 9. Analysis and comparison of a variety of soft computing methods found in the literature.

makes it simple to determine a method’s performance. Based on the data presented in the bar chart, the following outcomes about the FOA method can be drawn: It has the following desirable properties: (1) it is robust and reliable; (2) it has a straightforward design and can be easily programmed and compiled; (3) it can differentiate between LMPPs and GMPPs when running under PSC; (4) it converges quickly and does not exhibit steady-state oscillations.

B. STATISTICAL ANALYSIS

By applying quantitative analysis, such as the mean, maximum, and standard deviation of the PV power, this section makes a comparison between the performance of the proposed FOA algorithm and other MPPT algorithms that have already been developed. The mean was utilized in order to examine the exactness of the different MPPT algorithms while, the standard deviation was utilized in order to ascertain the level of dispersion that existed within the power data sets. Two nonparametric assessments, the Wilcoxon rank-sum and

TABLE 6. Wilcoxon rank-sum test statistical findings.

Shading Pattern	Algorithm	Power(W)			Rank-Sum
		Max	Mean	SD	
Pattern1	P&O	177.9	168	16.11	(+)
	PSO	179.75	145.8	18.37	(+)
	GWO	179.81	170.1	18.78	(+)
	FOA	179.9	174.9	17.66	(+)
Pattern2	P&O	29.32	25.43	7.62	(+)
	PSO	36.74	30.62	9.78	(+)
	GWO	37.21	33.56	3.27	(+)
	FOA	37.24	33.95	7.29	(+)
Pattern3	P&O	83.63	80.92	3.99	(+)
	PSO	87.33	79.15	14.17	(+)
	GWO	87.34	79.50	13.04	(+)
	FOA	87.37	82.09	12.34	(+)
Pattern4	P&O	53.62	34.88	5.26	(+)
	PSO	99.21	93.21	16.90	(+)
	GWO	99.26	81.6	22.06	(+)
	FOA	99.32	90.94	14.31	(+)

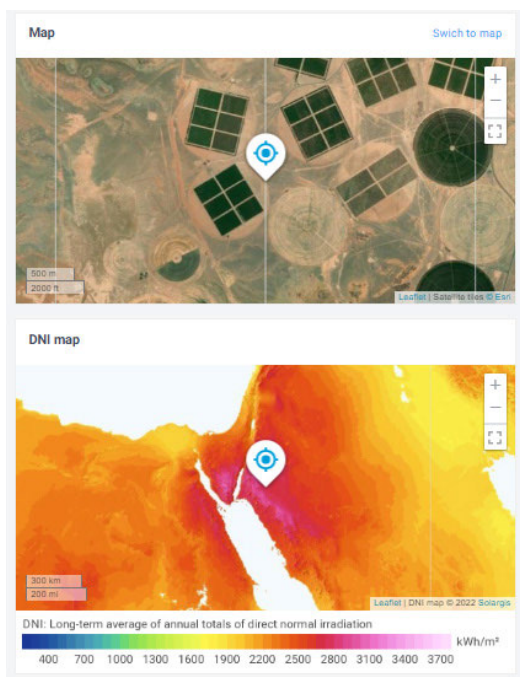


FIGURE 10. A Solar Atlas of Saudi Arabia (NEOM location).

the irradiance conditions. The primary cause of shadow is the obstruction of the direct irradiance component by an object, and the associated decrease in energy production may be observed more or less clearly. Fig. 12(a) shows the irradiation profile under a clear day in June, which compares the output of two solar panels that are physically close to one another and have micro-inverters installed. In the morning, one of the panels was covered with a shade (the green line). The difference in output caused by shadows is seen quite clearly

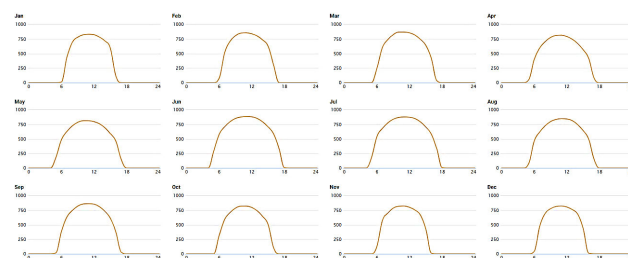
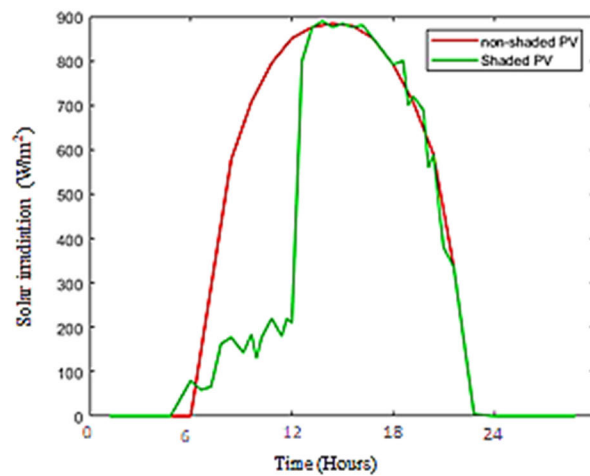
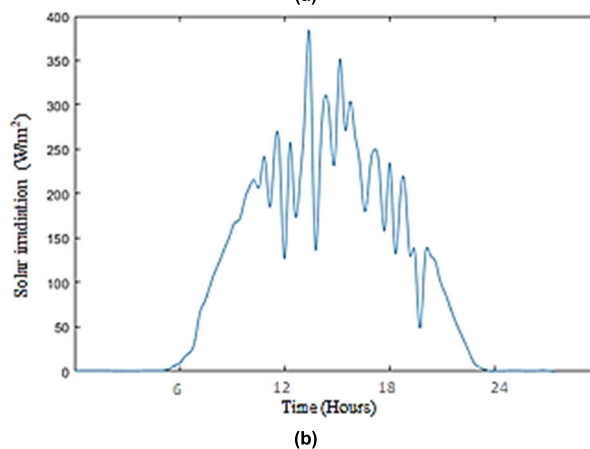


FIGURE 11. The intensity of solar irradiation varies during the period of the year [58].



(a)



(b)

FIGURE 12. Solar irradiation of (a) clear day of two PV panels shaded panel (green line) and unshaded panel (red line) (b) cloudy day [58], [59].

in the figure, which represents a day with clear conditions. Fig. 12(b) shows the irradiation profile under a cloudy day.

Using Atlas data, a simulation is run in real time to evaluate a 180W PV system. This data can be used to assess the dynamic efficiency of MPPT algorithms. The results of the test of the three MPPT algorithm under clear sky day are displayed in Fig.13. The results show that the power output from the FOA and traditional P&O are comparable, although the conventional P&O shifts away from the MPP at some points. However, the PSO method oscillates excessively during the

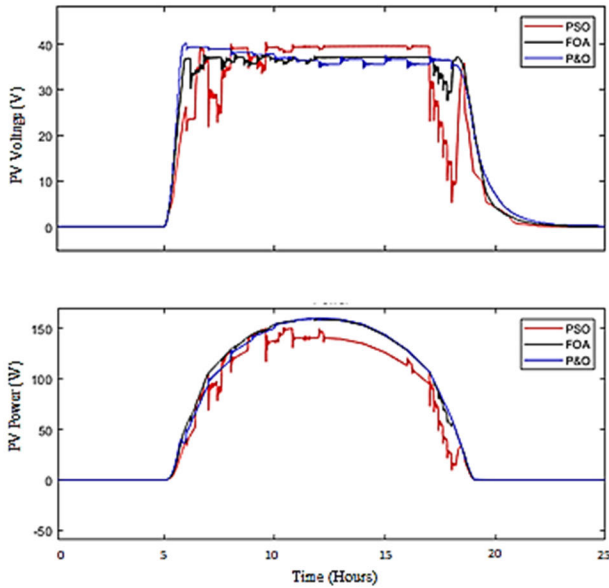


FIGURE 13. PV power and PV voltage of three MPPT methods under irradiation of clear day.

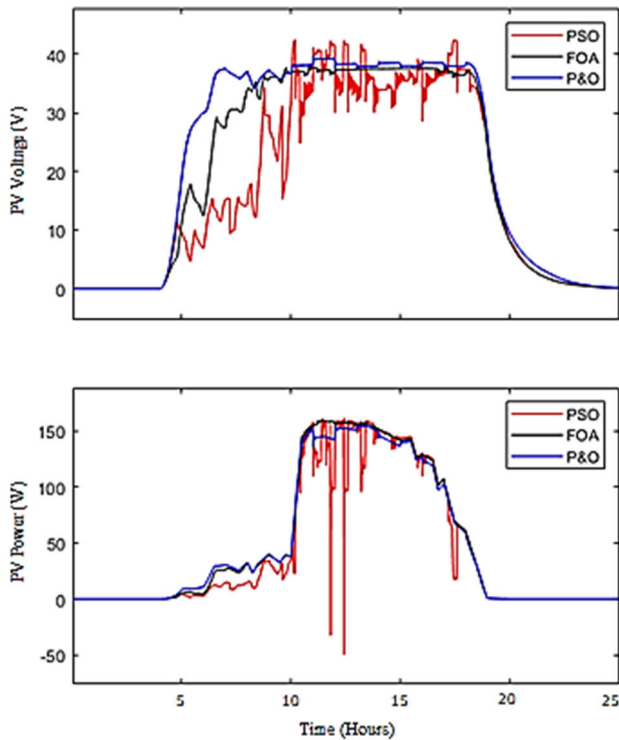


FIGURE 14. PV power and PV voltage of three MPPT methods under irradiation of clear day with one shaded panel.

tracking of GMPP. Fig. 14 shows the simulation results of the FOA method, P&O method, and PSO method when one of the PV panels is shaded (Fig. 12.(a)). It is clear that the P&O method has successive steady state oscillation in the PV power waveforms. The PSO method suffers from large oscillation while performing dynamic tracking. Fig. 15 shows

TABLE 7. Long-term tests were used to evaluate the proposed method's performance and the proposed GMPPT method's profitability.

Weather Condition	Tracking Method	Energy Extracted per Day (kWh)	Annual Energy (kWh)	Revenue in SR
Steady Change	P&O	10.506	126.074	22693.32
	PSO	16.50	198.00	35640
	Proposed	17.67	212.09	38176.2
Rapid Change	P&O	3.198	38.376	6907.7
	Proposed	5.157	61.884	11139

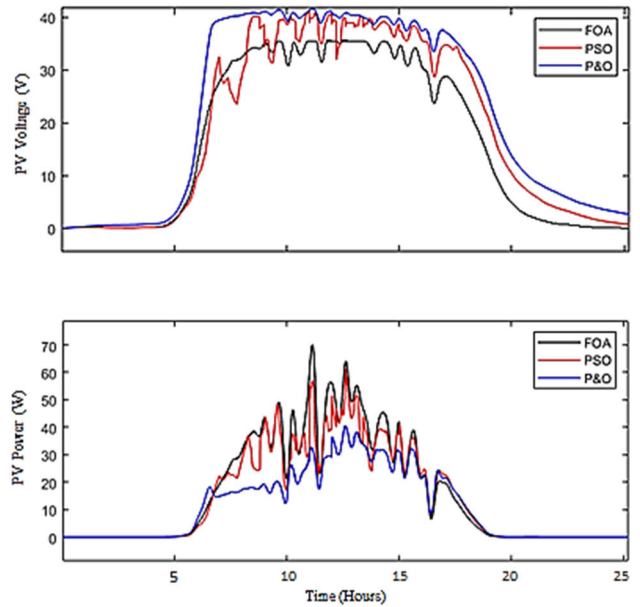


FIGURE 15. PV power and PV voltage of three MPPT methods under irradiation of cloudy day.

the simulation results when the system is tested under a cloudy day (Fig.12.(b)). The simulation results show that FOA method has good performance for dynamic tracking. However, the P&O method has bad performance, low PV output power, and low efficiency, resulting in huge losses in the PV system. The PSO method suffers from high switching transients while working under dynamic tracking. The overall outcome places the FOA method first, followed by other methods. This demonstrates without a doubt that FOA is among the most powerful methods that works for MPPT.

The numerical findings for the long-term test are shown in Table 7. The findings reveal the total power generated on a daily and annual basis, as well as the estimated income earned by applying a selling rate to the generated energy in Saudi Arabia in 2022 (0.18 SR per kWh). This demonstrates that proposed method may improve revenue and generate more extra income than the compared MPPT methods, which benefits the operating day. The proposed FOA may increase overall energy by 6.7% and 40.5% under steady change conditions compared to the PSO method and P&O method. In addition, it may increase overall energy by 11.6% and 38%

under rapid change conditions compared to the PSO method and P&O method. According to short-term testing, the proposed method's ability to work under PSC reduces power loss. In summary, short-term tests indicate that tracking speed might be enhanced, as seen by each track having a smaller power loss compared to other MPPT methods. As a result, when operated for a longer period of time using the proposed method, the amount of energy produced by the PV system increases.

VIII. CONCLUSION

In this study, a novel falcon optimization algorithm was employed to track the GMPP for the PV system. Analyses were performed on the output characteristics of the PV array while it was subjected to PSCs, and the operating concept of the proposed FOA was presented. In the study, the fundamental idea behind the FOA-based MPPT algorithm as well as its most important variables were discussed in depth. The proposed method has a high level of performance and is able to successfully track the GMPP under a variety of PSCs. Through the use of simulations, the FOA method's performance was evaluated and analyzed for verification purposes. According to the findings of the simulations, the FOA that was developed demonstrates greater performance when compared to the other MPPT algorithms. The proposed FOA has a fast tracking speed and its efficiency in tracking GMPP is greater than 99% across a wide range of different environmental conditions. The FOA is able to discern between a local peak and a global peak regardless of the shadow conditions that are present, as demonstrated by simulation tests that were carried out using four different shading conditions. In addition, an analysis of the proposed FOA in comparison to other soft computing methods found in the literature (based on the criteria given) was presented in Section VI. Specifically, the critical six factors that determine the system's performance were studied, and based on the information shown in the bar chart, FOA was ranked in top place, followed by GWO, PSO, ANN, and P&O. Also, the Friedman and Wilcoxon rank-sum tests demonstrate that FOA is significantly superior to the other MPPT methods evaluated. It is expected that PV researchers who are looking for an efficient operation of PV systems will be interested in the proposed FOA.

REFERENCES

- [1] F. Aminifar, M. Shahidehpour, A. Alabdulwahab, A. Abusorrah, and Y. Al-Turki, "The proliferation of solar photovoltaics: Their impact on widespread deployment of electric vehicles," *IEEE Electr. Mag.*, vol. 8, no. 3, pp. 79–91, Sep. 2020.
- [2] I. F. Silva, P. D. S. Vicente, F. L. Tofoli, and E. M. Vicente, "Plotting characteristic curves of photovoltaic modules: A simple and portable approach," *IEEE Ind. Appl. Mag.*, vol. 27, no. 3, pp. 63–72, Feb. 2021.
- [3] B. Subudhi and R. Pradhan, "A comparative study on maximum power point tracking techniques for photovoltaic power systems," *IEEE Trans. Sustain. Energy*, vol. 4, no. 1, pp. 89–98, Jan. 2013.
- [4] M. A. Elgendy, B. Zahawi, and D. J. Atkinson, "Assessment of perturb and observe MPPT algorithm implementation techniques for PV pumping applications," *IEEE Trans. Sustainable Energy*, vol. 3, no. 1, pp. 21–33, Jan. 2012.
- [5] M. A. Elgendy, B. Zahawi, and D. J. Atkinson, "Assessment of the incremental conductance maximum power point tracking algorithm," *IEEE Trans. Sustain. Energy*, vol. 4, no. 1, pp. 108–117, Jan. 2013.
- [6] A. Al Nabulsi and R. Dhaouadi, "Efficiency optimization of a DSP-based standalone PV system using fuzzy logic and dual-MPPT control," *IEEE Trans. Ind. Informat.*, vol. 8, no. 3, pp. 573–584, Aug. 2012.
- [7] S. B. Kjaer, "Evaluation of the 'hill climbing' and the 'incremental conductance' maximum power point trackers for photovoltaic power systems," *IEEE Trans. Energy Convers.*, vol. 27, no. 4, pp. 922–929, Dec. 2012.
- [8] N. Femia, G. Petrone, G. Spagnuolo, and M. Vitelli, "Optimization of perturb and observe maximum power point tracking method," *IEEE Trans. Power Electron.*, vol. 20, no. 4, pp. 963–973, Jul. 2005.
- [9] N. Femia, D. Granozio, G. Petrone, G. Spagnuolo, and M. Vitelli, "Predictive & adaptive MPPT perturb and observe method," *IEEE Trans. Aerosp. Electron. Syst.*, vol. 43, no. 3, pp. 934–950, Jul. 2007.
- [10] D. Sera, L. Mathe, T. Kerekes, S. V. Spataru, and R. Teodorescu, "On the perturb-and-observe and incremental conductance MPPT methods for PV systems," *IEEE J. Photovolt.*, vol. 3, no. 3, pp. 1070–1078, Jul. 2013.
- [11] T. Esram and P. L. Chapman, "Comparison of photovoltaic array maximum power point tracking techniques," *IEEE Trans. Energy Convers.*, vol. 22, no. 2, pp. 439–449, Jun. 2007.
- [12] S. Jain and V. Agarwal, "Comparison of the performance of maximum power point tracking schemes applied to single-stage gridconnected photovoltaic systems," *IET Electr. Power Appl.*, vol. 1, no. 5, pp. 753–762, Sep. 2007.
- [13] M. A. A. Mamun, M. Hasanuzzaman, and J. Selvaraj, "Experimental investigation of the effect of partial shading on photovoltaic performance," *IET Renew. Power Gener.*, vol. 11, no. 7, pp. 912–921, Jun. 2017.
- [14] A. Bidram, A. Davoudi, and R. S. Balog, "Control and circuit techniques to mitigate partial shading effects in photovoltaic arrays," *IEEE J. Photovolt.*, vol. 2, no. 4, pp. 532–546, Oct. 2012.
- [15] B. Yang, T. Zhu, J. Wang, H. Shu, T. Yu, X. Zhang, W. Yao, and L. Sun, "Comprehensive overview of maximum power point tracking algorithms of PV systems under partial shading condition," *J. Cleaner Prod.*, vol. 268, Sep. 2020, Art. no. 121983.
- [16] A. K. Podder, N. K. Roy, and H. R. Pota, "MPPT methods for solar PV systems: A critical review based on tracking nature," *IET Renew. Power Gener.*, vol. 13, no. 10, pp. 1615–1632, Jul. 2019.
- [17] R. Guruambeth and R. Ramabadrhan, "Fuzzy logic controller for partial shaded photovoltaic array fed modular multilevel converter," *IET Power Electron.*, vol. 9, no. 8, pp. 1694–1702, Jun. 2016.
- [18] V. R. Kota and M. N. Bhukya, "A novel global MPP tracking scheme based on shading pattern identification using artificial neural networks for photovoltaic power generation during partial shaded condition," *IET Renew. Power Gener.*, vol. 13, no. 10, pp. 1647–1659, Apr. 2019.
- [19] M. Miyatake, M. Veerachary, F. Toriumi, N. Fujii, and H. Ko, "Maximum power point tracking of multiple photovoltaic arrays: A PSO approach," *IEEE Trans. Aerosp. Electron. Syst.*, vol. 47, no. 1, pp. 367–380, Jan. 2011.
- [20] K. Ishaque, Z. Salam, M. Amjad, and S. Mekhilef, "An improved particle swarm optimization (PSO)-based MPPT for PV with reduced steady-state oscillation," *IEEE Trans. Power Electron.*, vol. 27, no. 8, pp. 3627–3638, Aug. 2012.
- [21] K. Sundareswaran, S. Peddapati, and S. Palani, "MPPT of PV systems under partial shaded conditions through a colony of flashing fireflies," *IEEE Trans. Energy Convers.*, vol. 29, no. 2, pp. 463–472, Jun. 2014.
- [22] S. Mohanty, B. Subudhi, and P. K. Ray, "A new MPPT design using grey wolf optimization technique for photovoltaic system under partial shading conditions," *IEEE Trans. Sustain. Energy*, vol. 7, no. 1, pp. 181–188, Jan. 2016.
- [23] K. Kaced, C. Larbes, N. Ramzan, M. Bounabi, and Z. E. Dahmane, "Bat algorithm based maximum power point tracking for photovoltaic system under partial shading conditions," *Sol. Energy*, vol. 158, pp. 490–503, Dec. 2017.
- [24] J. P. Ram and N. Rajasekar, "A new global maximum power point tracking technique for solar photovoltaic (PV) system under partial shading conditions (PSC)," *Energy*, vol. 118, no. 1, pp. 512–525, Jan. 2017.
- [25] J. Ahmed and Z. Salam, "A maximum power point tracking (MPPT) for PV system using cuckoo search with partial shading capability," *Appl. Energy*, vol. 119, pp. 118–130, Apr. 2014.
- [26] M. Kermadi, Z. Salam, J. Ahmed, and E. M. Berkouk, "A high-performance global maximum power point tracker of PV system for rapidly changing partial shading conditions," *IEEE Trans. Ind. Electron.*, vol. 68, no. 3, pp. 2236–2245, Mar. 2021.

- [27] D. Yousri, T. S. Babu, D. Allam, V. K. Ramachandaramurthy, E. Beshr, and M. B. Eteiba, "Fractional chaos maps with flower pollination algorithm for partial shading mitigation of photovoltaic systems," *Energies*, vol. 12, no. 18, p. 3548, Sep. 2019.
- [28] O. Abdalla, H. Rezk, and E. M. Ahmed, "Wind driven optimization algorithm based global MPPT for PV system under non-uniform solar irradiance," *Sol. Energy*, vol. 180, pp. 429–444, Mar. 2019.
- [29] K. S. Tey, S. Mekhilef, H.-T. Yang, and M.-K. Chuang, "A differential evolution based MPPT method for photovoltaic modules under partial shading conditions," *Int. J. Photoenergy*, vol. 2014, pp. 1–10, May 2014.
- [30] S. Hadji, J.-P. Gaubert, and F. Krim, "Theoretical and experimental analysis of genetic algorithms based MPPT for PV systems," *Energy Proc.*, vol. 74, pp. 772–787, Aug. 2015.
- [31] L. Guo, Z. Meng, Y. Sun, and L. Wang, "A modified cat swarm optimization based maximum power point tracking method for photovoltaic system under partially shaded condition," *Energy*, vol. 144, pp. 501–514, Feb. 2018.
- [32] H. Yatimi and E. Aroudam, "Assessment and control of a photovoltaic energy storage system based on the robust sliding mode MPPT controller," *Sol. Energy*, vol. 139, pp. 557–568, Dec. 2016.
- [33] M. Kermadi, V. J. Chin, S. Mekhilef, and Z. Salam, "A fast and accurate generalized analytical approach for PV arrays modeling under partial shading conditions," *Sol. Energy*, vol. 208, pp. 753–765, Sep. 2020.
- [34] I. Shams, S. Mekhilef, and K. S. Tey, "Maximum power point tracking using modified butterfly optimization algorithm for partial shading, uniform shading, and fast varying load conditions," *IEEE Trans. Power Electron.*, vol. 36, no. 5, pp. 5569–5581, May 2021.
- [35] M. Mansoor, A. F. Mirza, Q. Ling, and M. Y. Javed, "Novel grass hopper optimization based MPPT of PV systems for complex partial shading conditions," *Sol. Energy*, vol. 198, pp. 499–518, Mar. 2020.
- [36] J. P. Ram, D. S. Pillai, A. M. Y. M. Ghias, and N. Rajasekar, "Performance enhancement of solar PV systems applying P&O assisted flower pollination algorithm (FPA)," *Sol. Energy*, vol. 199, pp. 214–229, Mar. 2020.
- [37] Z. Wang, N. Das, A. Helwig, and T. Ahfock, "Modeling of multi-junction solar cells for maximum power point tracking to improve the conversion efficiency," in *Proc. Australas. Universities Power Eng. Conf. (AUPEC)*, Nov. 2017, pp. 1–6, doi: 10.1109/AUPEC.2017.8282402.
- [38] D. Yousri, T. S. Babu, D. Allam, V. K. Ramachandaramurthy, E. Beshr, and M. B. Eteiba, "Fractional chaos maps with flower pollination algorithm for partial shading mitigation of photovoltaic systems," *Energies*, vol. 12, no. 18, p. 3548, Sep. 2019.
- [39] D. K. Mathi and R. Chinthamalla, "Enhanced leader adaptive velocity particle swarm optimisation based global maximum power point tracking technique for a PV string under partially shaded conditions," *IET Renew. Power Gener.*, vol. 14, no. 2, pp. 243–253, Feb. 2020.
- [40] A. M. Eltamaly, M. S. Al-Saud, and A. G. Abokhalil, "A novel bat algorithm strategy for maximum power point tracker of photovoltaic energy systems under dynamic partial shading," *IEEE Access*, vol. 8, pp. 10048–10060, 2020.
- [41] A. M. Eltamaly, M. S. Al-Saud, A. G. Abokhalil, and H. M. H. Farh, "Simulation and experimental validation of fast adaptive particle swarm optimization strategy for photovoltaic global peak tracker under dynamic partial shading," *Renew. Sustain. Energy Rev.*, vol. 124, May 2020, Art. no. 109719.
- [42] N. Priyadarshi, S. Padmanaban, J. B. Holm-Nielsen, F. Blaabjerg, and M. S. Bhaskar, "An experimental estimation of hybrid ANFIS–PSO-based MPPT for PV grid integration under fluctuating sun irradiance," *IEEE Syst. J.*, vol. 14, no. 1, pp. 1218–1229, Mar. 2020.
- [43] N. Priyadarshi, S. Padmanaban, P. K. Maroti, and A. Sharma, "An extensive practical investigation of FPSO-based MPPT for grid integrated PV system under variable operating conditions with anti-islanding protection," *IEEE Syst. J.*, vol. 13, no. 2, pp. 1861–1871, Jun. 2019.
- [44] D. Pilakkat and S. Kanthalakshmi, "An improved P&O algorithm integrated with artificial bee colony for photovoltaic systems under partial shading conditions," *Sol. Energy*, vol. 178, pp. 37–47, Jan. 2019.
- [45] M. Mao, L. Zhou, Z. Yang, Q. Zhang, C. Zheng, B. Xie, and Y. Wan, "A hybrid intelligent GMPPT algorithm for partial shading PV system," *Control Eng. Pract.*, vol. 83, pp. 108–115, Feb. 2019.
- [46] M. Seyedmahmoudian, R. Rahmani, S. Mekhilef, A. M. T. Oo, A. Stojcevski, T. K. Soon, and A. S. Ghandhari, "Simulation and hardware implementation of new maximum power point tracking technique for partially shaded PV system using hybrid DEPSO method," *IEEE Trans. Sustain. Energy*, vol. 6, no. 3, pp. 850–862, Jul. 2015.
- [47] E. H. de Vasconcelos Segundo, V. C. Mariani, and L. D. S. Coelho, "Design of heat exchangers using falcon optimization algorithm," *Appl. Thermal Eng.*, vol. 156, pp. 119–144, Jun. 2019.
- [48] V. Tucker, "Gliding flight: Speed and acceleration of ideal falcons during diving and pull out," *J. Experim. Biol.*, vol. 201, no. 3, pp. 403–414, Feb. 1998.
- [49] V. A. Tucker, "Gliding flight: Drag and torque of a hawk and a falcon with straight and turned heads, and a lower value for the parasite drag coefficient," *J. Experim. Biol.*, vol. 203, no. 24, pp. 3733–3744, Dec. 2000.
- [50] T. S. Babu, N. Rajasekar, and K. Sangeetha, "Modified particle swarm optimization technique based maximum power point tracking for uniform and under partial shading condition," *Appl. Soft Comput.*, vol. 34, pp. 613–624, Sep. 2015.
- [51] S. N. Deshkar, S. B. Dhale, J. S. Mukherjee, T. S. Babu, and N. Rajasekar, "Solar PV array reconfiguration under partial shading conditions for maximum power extraction using genetic algorithm," *Renew. Sustain. Energy Rev.*, vol. 43, pp. 102–110, Mar. 2015.
- [52] T. R. Gadekallu and N. Khare, "Cuckoo search optimized reduction and fuzzy logic classifier for heart disease and diabetes prediction," *Int. J. Fuzzy Syst. Appl.*, vol. 6, no. 2, pp. 25–42, Apr. 2017.
- [53] A. Gandomi, *Metaheuristic Applications in Structures and Infrastructures*. London, U.K.: Elsevier, 2013.
- [54] S. Mirjalili, S. Mirjalili, and A. Lewis, "Grey wolf optimizer," in *Proc. Adv. Eng. Softw.*, vol. 69, 2014, pp. 46–61.
- [55] A. Hedenstrom, M. Rosen, S. Akesson, and F. Spina, "Flight performance during hunting excursions in Eleonora's falcon *Falco eleonora*," *J. Experim. Biol.*, vol. 202, no. 15, pp. 2029–2039, Aug. 1999.
- [56] Texas Instruments. *Application Note Basic Calculation of a Boost Converter's Power Stage*. Accessed: Nov. 14, 2022. [Online]. Available: <http://www.ti.com/lit/an/slva372d/slva372d.pdf?ts=1668413830595>
- [57] *Solar Direct, Where the World Shops for Energy*. Accessed: Nov. 14, 2022. [Online]. Available: <https://shop.solardirect.com/>
- [58] *Global Solar Atlas*. Accessed: Nov. 15, 2022. [Online]. Available: <https://globalsolaratlas.info/map?c=27.88794,36.650806,8&s=28.522045,35.385324&m=site>
- [59] R. A. Shalwala, J. Bleijs, and P. Lefley, "PV integration into distribution networks in Saudi Arabia," M.S. thesis, Dept. Eng., Univ. Leicester, Leicester, U.K., 2012.



MUHANNAD J. ALSHAREEF was born in Riyadh, Saudi Arabia, in 1988. He received the B.Sc. degree in electrical engineering from Umm Al-Qura University, Saudi Arabia, in 2011, the M.Sc. degree in electronics and electrical engineering from Coventry University, U.K., in 2016, and the Ph.D. degree in electrical engineering from Aston University, U.K., in 2019. Since 2020, he has been an Assistant Professor with the College of Electronic and Communication Engineering, Umm Al-Qura University. His research interests include photovoltaic modeling and control, intelligent control, nonlinear systems control, and optimization techniques, such as genetic algorithm, particle swarm optimization, and control and protection of dc microgrid.

...